NASA TN D-4689

ANALYSIS AND MECHANIZATION OF THREE- AND FOUR-GIMBAL SYSTEMS

By John W. Wilson

Langley Research Center
Langley Station, Hampton, Va.

NATIONAL AERONAUTICS AND SPACE ADMINISTRATION

For sale by the Clearinghouse for Federal Scientific and Technical Information
Springfield, Virginia 22151 – CFSTI price $3.00

ANALYSIS AND MECHANIZATION OF THREE- AND FOUR-GIMBAL SYSTEMS

By John W. Wilson
Langley Research Center

SUMMARY

An approximate algebraic technique which extends the usefulness of three-gimbal systems is presented. In analyzing the three-gimbal problem, the Euler angles are explored about the singular points and are found to be, in general, non-unique. This non-uniqueness is eliminated by minimizing the magnitude of the discontinuities at the singular points. An approximate mathematical model of the inverse Euler angle problem is developed which chooses the solution with minimum discontinuity and, in addition, replaces high rates over large angles by small discontinuities. A computer circuit is devised for this model.

A proposed four-gimbal system is investigated and a mathematical model is derived by finding a necessary differential constraint on the fourth angle to maintain a nonsingular formulation. This constraint is then used to derive a particular mathematical formulation in an essentially algebraic form, from which a computer circuit is developed. The rate equations of the four angles are also derived. Existing four-gimbal stable platforms are analyzed and discussed.

INTRODUCTION

Three-gimbal systems have been used for several years as a means of displaying visual information in flight simulation. Traditionally the Euler angles, needed to drive these gimbals, were also used in the main calculations as parameters of rotation from which the direction cosine matrix was computed. Difficulties with the singular points were normally avoided since only small portions of the flight program were studied. Thus, gimbal systems could be chosen with gimbal lock out of the region of interest.

As the need to study highly maneuverable fighter aircraft and spacecraft arose, the trend was to remove the errors due to singularities from the main calculations by using either the Euler parameters or direction cosine rate equations. The Euler angles were then determined algebraically from the direction cosines (ref. 1, pp. 415-418). Although

the main calculations did not suffer from the singularities, little concern was given to the resultant positioning errors of the visual display system (ref. 2).

The newest concept in flight simulation is the full-mission simulator. This concept has had a tremendous impact on both simulation computing practices and visual display hardware design. Present-day full-mission simulators require complete freedom of rotation of the coordinate axes with the ability to hold at any altitude for indefinite periods and angular drives for several orders of rotation between several different such coordinate axes. To meet these requirements, an algebraic computation is a must in order to synchronize the motion, and considerable care must be maintained in the computation of the transformation matrices between these various axis systems. Still an open question is the method to determine the Euler angles in the neighborhood of the singular points.

The behavior at the singular points is not a serious consequence until mechanical equipment (namely, a three gimbal) is required to track the motion. Then consideration should be given to minimizing the dynamic positioning error due to rate limiting of the gimbal system. The purpose of this report is to develop a simple method by which the positioning errors can be reduced. In minimizing the dynamic positioning error, it is found that a static error is introduced in the neighborhood of the singular points. This method contains an adjustable parameter in the form of a dead band about the singular points. A value for the dead band, within computer capabilities, can be chosen which best meets the mission requirements without driving the gimbal far beyond its response limitations.

Even though the method established in this report can reduce the positioning errors associated with the singularities of the three-gimbal system, some rate limiting and static error still exist in the neighborhood of the singular points. A four-gimbal system can remove these difficulties. In this paper are presented the development of a mathematical model for a specific four-gimbal system and the results of simple experiments to demonstrate its operation. A reasonable amount of ingenuity should allow extension of this analysis to any general four-gimbal configuration.

With the increased capability of modern aircraft and spacecraft, flight situation indicators that can adequately display attitudes of the vehicles are required. To meet this need, four-gimbal stabilized platforms have been proposed (refs. 3 and 4). However, the methods proposed to drive these systems yield discontinuities similar to those encountered in three-gimbal systems. When these discontinuities occur, the corresponding gimbal drives must be delicately balanced to assure platform isolation. These systems are analyzed herein and the cause of these discontinuities is ascertained.

SYMBOLS

Function:

A(t)	transformation matrix from fixed-coordinate frame to rotating-coordinate frame, dimensionless
a_{ij}	elements of A(t), where subscripts i and j = 1, 2, or 3, dimensionless
a,b,c,d	Euler parameters of rotation of rotating-coordinate frame with respect to fixed-coordinate frame, dimensionless
$C\gamma$	cosine of any angle γ, dimensionless
K	positive gain constant
k,ℓ,m,n	integers
p,q,r	components of angular velocity vector of rotating-coordinate frame with respect to fixed-coordinate frame, measured along rotating coordinate axes, radians/second
$S\gamma$	sine of any angle γ, dimensionless
sgn( )	signum function, equal to +1 for variable ≥ 0 and -1 for variable <0, dimensionless
t	time, seconds
$\overline{V}_f$	vector measured in coordinate frame considered fixed, arbitrary units
$\overline{V}_r$	vector measured in coordinate frame considered rotating, arbitrary units
$[\gamma]_\lambda$	transformation matrix of a simple rotation through any angle γ about any axis λ, dimensionless; that is,

$$[\gamma]_X = \begin{bmatrix} 1 & 0 & 0 \\ 0 & C\gamma & S\gamma \\ 0 & -S\gamma & C\gamma \end{bmatrix}; \quad [\gamma]_Y = \begin{bmatrix} C\gamma & 0 & -S\gamma \\ 0 & 1 & 0 \\ S\gamma & 0 & C\gamma \end{bmatrix}; \quad [\gamma]_Z = \begin{bmatrix} C\gamma & S\gamma & 0 \\ -S\gamma & C\gamma & 0 \\ 0 & 0 & 1 \end{bmatrix}$$

$[\gamma]_\lambda$ — inverse or transpose of $[\gamma]_\lambda$, dimensionless

ϕ,θ,ψ — Euler angles relating fixed frame to rotating frame in three-gimbal system (bank angle, pitch angle, and heading), radians

α,ϕ,θ,ψ — angles relating fixed frame to rotating frame in four-gimbal system (for $\alpha = 0$, ϕ is bank angle, θ is pitch angle, and ψ is heading), radians

ω_L — maximum slew rate of gimbal system, radians/second

$\overline{\omega}$ — angular velocity vector of rotating-coordinate frame with respect to fixed-coordinate frame, radians/second

$\overline{\omega}_G$ — $\overline{\omega}$ measured in three-gimbal space, radians/second

Subscripts:

o — value at $t = 0$

\+ — signifies right-hand limit

\- — signifies left-hand limit

Dot over symbol indicates derivative with respect to time.

Computer:

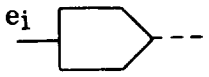

servomotor that turns shaft in direction of input voltage

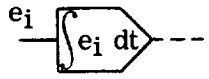

integrating servomotor that turns shaft proportionally to integral of input voltage

potentiometer whose output voltage is K times input voltage

inverting amplifier whose output voltage is the negative of input voltage

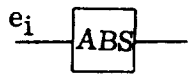

absolute value circuit whose output voltage is equal to magnitude of input voltage

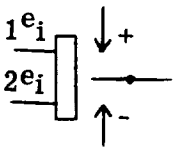

relay such that, if the sum of input voltages is negative, the switch is in the - position and in the + position otherwise

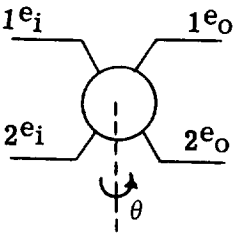

shaft driven resolver whose output voltages are

$1e_o = 1e_i \cos\theta - 2e_i \sin\theta$

$2e_o = 2e_i \cos\theta + 1e_i \sin\theta$

where θ is shaft rotation

THE THREE-GIMBAL PROBLEM

Analysis

The order of the Euler angles (fig. 1) considered in this analysis is that of the conventional airplane angles ψ, θ, and ϕ. It is assumed that the transformation matrix A(t) is available as a function of time and is defined by

$$\overline{V}_r = A(t)\overline{V}_f \tag{1}$$

The transformation matrix was generated by the Euler parameters given by equations (A1) and (A2) in appendix A.

The transformation matrix A(t) uniquely defines the relative orientation of the two coordinate frames as a function of time. The Euler angles are then related to the elements of A(t) as

$$[\phi]_X[\theta]_Y[\psi]_Z = A(t) \tag{2}$$

The inverse Euler angle problem is to solve these functional relations for the three angles (that is, mapping of the elements of A(t) into ψ, θ, and ϕ). Equation (2) is expanded in

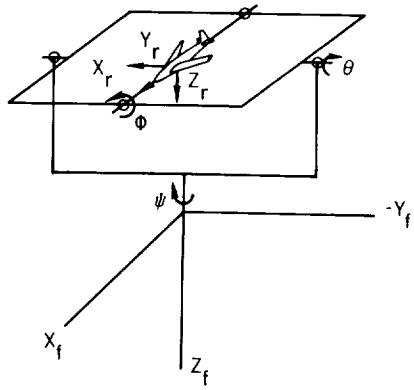

Figure 1.- Three-gimbal configuration considered in the analysis.

equation (A3) of appendix A. The inverse problem is seen to be everywhere non-unique[1] since

$$[\phi \pm \pi]_X[\pi - \theta]_Y[\psi \pm \pi]_Z = A(t) \tag{3}$$

The inverse of the mapping exists and is locally one-to-one when the Jacobian does not vanish (ref. 5, pp. 225-232), otherwise it is said to be singular. As $\cos\theta$ approaches zero, the Jacobian of the inverse problem vanishes; that is, no three elements of $A(t)$ can be found such that

$$\left.\frac{\partial(a_{ij},a_{kl},a_{mn})}{\partial(\psi,\theta,\phi)}\right|_{\cos\theta=0} \neq 0$$

where

$$i,j,k,l,m,n = 1, 2, \text{ or } 3$$

Hence, a functional dependence exists between ψ and ϕ. This functional relation is found from equation (2) as $\cos\theta$ approaches zero and $\sin\theta$ approaches ± 1 to be

$$\begin{bmatrix} 0 & 0 & \mp 1 \\ \pm S(\phi \mp \psi) & C(\phi \mp \psi) & 0 \\ \pm C(\phi \mp \psi) & -S(\phi \mp \psi) & 0 \end{bmatrix} = A(t) \tag{4}$$

An alternate method of computing the Euler angles is the following Euler angle rate equations (ref. 1, p. 351):

$$\dot{\psi} = \frac{rC\phi + qS\phi}{C\theta} \tag{5}$$

$$\dot{\theta} = qC\phi - rS\phi \tag{6}$$

$$\dot{\phi} = p + \dot{\psi}S\theta \tag{7}$$

The solution to the rate equations is unique on intervals not containing the singular points. If a singular point is encountered, uniqueness is no longer assured. It is shown later that, as $\cos\theta$ approaches zero, equation (5) is indeterminate. At the singular points, $\sin\theta = \pm 1$, equation (7) can be rewritten (ref. 6) as

$$\phi \mp \psi = \int p\, dt \tag{8}$$

---

[1]Non-uniqueness is restricted herein to solutions within $\pm\pi$ of the principal solution.

Indicative of both the inverse problem and the rate formulation at the singular points is the functional dependence of ψ and ϕ; these angles are not defined at the singular points but either the sum (at $\sin\theta = -1$) or difference (at $\sin\theta = +1$) is defined. On every interval not containing a singular point, each solution of the inverse problem satisfies equations (5) to (7). The solution to the rate equations cannot be propagated uniquely through the singular points, but every set of functions which satisfy equations (5) to (7) except at the singular points will correspond to the solutions to the inverse problem. Hence, the analysis of one formulation discloses the behavior of the other.

The remainder of the analysis relies heavily on the principle of invariance. A transformation (of a vector) of invariance is such that if the components of the vector are transformed invariantly, then the vector is unchanged (that is, the transformation does not alter its magnitude or direction).

Consider the space with three coordinate axes defined by the directions of increasing ϕ, θ, and ψ shown in figure 2. These directions are the same as those of the gimbal axes shown in figure 1. The angular velocity vector $\bar{\omega}_G$, referenced to this oblique three-dimensional space, is given by

$$\bar{\omega}_G = T\bar{\omega} \tag{9}$$

The angular velocity vector $\bar{\omega}$ is referenced to a three-dimensional orthogonal space with components p, q, and r. The transformation T transforms from the orthogonal three-dimensional space to an oblique three-dimensional space with coordinates $\dot{\psi}$, $\dot{\theta}$, and $\dot{\phi}$ as shown in figure 2. Using equations (5) to (7) with equation (9) gives

$$\begin{bmatrix} \dot{\psi} \\ \dot{\theta} \\ \dot{\phi} \end{bmatrix} = \begin{bmatrix} 0 & \frac{S\phi}{C\theta} & \frac{C\phi}{C\theta} \\ 0 & C\phi & -S\phi \\ 1 & \frac{S\theta S\phi}{C\theta} & \frac{S\theta C\phi}{C\theta} \end{bmatrix} \begin{bmatrix} p \\ q \\ r \end{bmatrix} \tag{10}$$

As seen from figure 2, the obliqueness of the space depends on the angle θ. In the limit as $|\theta| \to \pi/2$, the oblique three-dimensional space collapses into a two-dimensional orthogonal space which is capable of representing only angular velocities that lie in the plane of the space; only the projection of a general vector in the three-dimensional space onto the two-dimensional space can be represented as seen in figure 3. (Note that the two-dimensional space coincides with the plane of the gimbal at gimbal lock.)

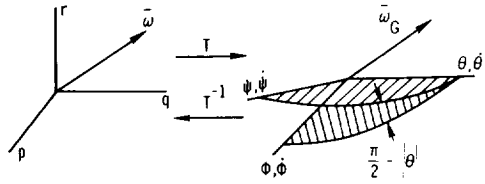

Figure 2.- Ordinary three-dimensional space and oblique three-dimensional space related through transformation T.

If invariance of the angular velocity vector under change of representation is required for every value of θ except for $|\theta| = \pi/2$, then the angular velocity vector must lie in the plane of the space (that is, in the limit as $|\theta|$ approaches $\pi/2$). In the limit as the singular point is approached, the out-of-plane component must vanish. The left-hand limit (time increasing) and the right-hand limit (time decreasing) are, in general, not equal (that is, the solution is discontinuous). This limiting process can be loosely viewed geometrically; if an angular velocity vector "appears" that does not lie in the planar space, then the space must rotate instantaneously to contain the vector.

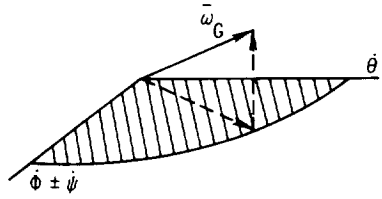

Figure 3.- Oblique three-dimensional space collapsed to a two-dimensional orthogonal space at singular points. The in-plane and out-of-plane components of a general vector in three-dimensional space are shown.

The qualitative behavior at the singular points is established. In order to look at the limiting process, the problem is reformulated explicitly in terms of the out-of-plane and in-plane components by rewriting equations (5), (6), and (7) as

$$\begin{bmatrix} \dot{\phi} - \dot{\psi}S\theta \\ \dot{\theta} \\ \dot{\psi}C\theta \end{bmatrix} = \begin{bmatrix} 1 & 0 & 0 \\ 0 & C\phi & -S\phi \\ 0 & S\phi & C\phi \end{bmatrix} \begin{bmatrix} p \\ q \\ r \end{bmatrix} \tag{11}$$

The vector on the left-hand side of equation (11) is referenced to a three-dimensional orthogonal space. Let the components be x', y', and z', where the z'-component is recognized as the out-of-plane component in the limit as indicated in figure 4.

Figure 4 shows the three-dimensional space with components x', y', and z' (at the singular points) in relation to the three-dimensional space with components p, q, and r to which $\bar{\omega}$ is referenced. The transformation from p,q,r to x',y',z' is given by

$$\begin{bmatrix} x' \\ y' \\ z' \end{bmatrix} = \begin{bmatrix} 1 & 0 & 0 \\ 0 & C\phi & -S\phi \\ 0 & S\phi & C\phi \end{bmatrix} \begin{bmatrix} p \\ q \\ r \end{bmatrix} \tag{12}$$

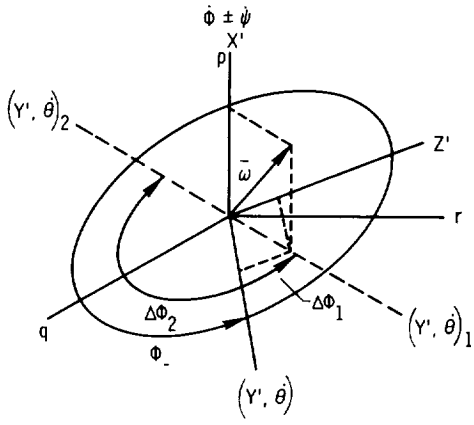

Figure 4.- The two-dimensional space (X'Y'-plane) is shown in relation to pqr space. The z'-component is the out-of-plane component that must be reduced to zero by the indicated discontinuous rotations.

At the singular points, the X'Y'-plane is the planar space of the gimbal shown in figure 3. The left-hand limit of the solution ϕ_- as the singular point is approached is shown as the angle between the $(Y', \dot{\theta})$ and the q axes. After the singular point is encountered there are two solutions corresponding to $(Y', \dot{\theta})_1$ and $(Y', \dot{\theta})_2$ for which the right-hand limit (time decreasing) of the out-of-plane

component vanishes, where $\overline{\omega}$ in figure 4 is the angular velocity vector at the exit (right-hand limit) from the neighborhood of the singular point. The right-hand limit of the out-of-plane component of the angular velocity vector is

$$z' = q_+ \sin \phi_+ + r_+ \cos \phi_+ = 0 \tag{13}$$

which is the numerator of equation (5). Hence, $\dot{\psi}$ is indeterminate. Equation (13) has two principal solutions corresponding to $\Delta\phi_1$ and $\Delta\phi_2$ in figure 4, which are the angles the space must be rotated instantaneously to contain the angular velocity vector. From figure 4, therefore,

$$\Delta\phi_1 = \pi - \Delta\phi_2 \tag{14}$$

As shown by equation (14), one discontinuity always has a magnitude less than or equal to $\pi/2$. As indicated by equations (4) and (8) a corresponding discontinuity occurs in ψ.

From this analysis, the following properties are noted:

(1) The angles ψ and ϕ are not defined at the singular points but either the sum or difference is defined. Hence, the angles can be chosen arbitrarily, subject to the preservation of equations (4) and (8).

(2) In general, discontinuities appear at the singular points but a discontinuity can be chosen to be $\pi/2$ or less in magnitude.

Application

A method is presented for computing the Euler angles from the elements of A(t). The Euler angles are functionally related to A(t) by equation (2). The non-uniqueness shown by equation (3) is used in minimizing the discontinuities at the singular points. The angle ϕ can be computed from a_{23} and a_{33} (eq. (A3), appendix A) by using a bootstrap (iterative) approach which makes $\cos \theta$ available as

$$\sin \phi = \frac{a_{23}}{\cos \theta} \qquad (\cos \theta \neq 0) \tag{15}$$

$$\cos \phi = \frac{a_{33}}{\cos \theta} \qquad (\cos \theta \neq 0) \tag{16}$$

With this knowledge of ϕ, a new matrix B(t) can be defined as

$$B(t) = \left[-\phi\right]_X A(t) \tag{17}$$

This matrix is functionally related to ψ and θ by

$$B(t) = [\theta]_Y[\psi]_Z \tag{18}$$

Equations (17) and (18) are expanded in appendix A. The solution of equation (18) is well defined, the form being that of the familiar two-gimbal problem.

The difficulties are left in the solutions of equations (15) and (16) when $\cos\theta$ is near zero and in minimizing the discontinuities. To circumvent these difficulties, the two properties summarized in the analysis are used.

A small dead band is established about the singular points within which ϕ is held (by property (1)) at the value computed by equations (15) and (16) at the entrance to the dead region (the left-hand limit of ϕ). The computation of ψ and θ from equation (18) insures the preservation of equations (4) and (8) at the singular points. If a roll maneuver ($p \neq 0$) is initiated in the dead region, an effective roll occurs through the ψ angle and the visual display moves in the proper direction.

As noted in the analysis, the discontinuities can be chosen to be $\pi/2$ or less (property (2)). The magnitude of the discontinuities must be computed so that the proper choice can be made. To compute the discontinuities, the left- (time increasing) and right-hand (time decreasing) limits of the solution as the singular points are approached must be found. The left-hand limit ϕ_- is computed by equations (15) and (16) upon entrance to the neighborhood of the singular points. With this value and the element b_{33} of equation (18), $\cos\theta$ is computed from

$$b_{33} = \cos\theta = a_{23}\sin\phi_- + a_{33}\cos\phi_- \tag{19}$$

The current value of ϕ is contained in a_{23} and a_{33} due to the following functional form:

$$a_{23} = \cos\theta\sin\phi_+ \tag{20}$$

$$a_{33} = \cos\theta\cos\phi_+ \tag{21}$$

Hence, when ϕ is discontinuous, equation (19) becomes

$$b_{33} = \cos\theta\cos\Delta\phi \tag{22}$$

where

$$\Delta\phi = \phi_+ - \phi_- \tag{23}$$

is the discontinuity.

Maintaining

$$|\Delta\phi| \leq \frac{\pi}{2} \tag{24}$$

provides the necessary choice between the solutions given by equations (2) and (3) (that is, $\cos\theta$ or $\cos(\pi - \theta) = -\cos\theta$) which minimizes the discontinuities. Hence, the choice

$$\text{sgn}(\cos\theta) = \text{sgn}(b_{33}) = \text{sgn}(\cos\theta)\text{sgn}(\cos\Delta\phi) \tag{25}$$

completes the necessary logic for a solution that minimizes discontinuities since equation (25) implies that

$$\text{sgn}(\cos\Delta\phi) = +1 \tag{26}$$

which indeed reflects inequality (24).

The dead band has the effect of introducing a static error and limiting the maximum angular rates of ψ and ϕ except, of course, for the discontinuities, the magnitudes of which will be minimized. Hence, there is a trade-off between static error and error due to rate limiting of mechanical equipment by choice of the size of the dead band.

Mechanization

Mechanizing the problem as formulated in the previous section can be accomplished in many ways. The method utilized herein uses the resolver chain described in reference 7. This mechanization is shown in figure 5. In the figure, the dead band (DB) is detected by

$$|a_{23}| + |a_{33}| = \left(|\cos\phi| + |\sin\phi|\right)|\cos\theta|$$

which gives a measure of $|\cos\theta|$. Note that $|a_{13}| = |\sin\theta|$ could have been used as well. When in the dead region the ϕ resolver is physically turned off by removing the power supply from the motor windings, as indicated in figure 5. The error signal to the ϕ resolver has its sign determined by $\text{sgn}(\cos\theta\cos\Delta\phi)$ which provides the minimization of discontinuities when the ϕ resolver is again made active. Inasmuch as the θ and ψ calculations are not directly affected by the dead band, equation (8) is preserved within a small error inside the dead region.

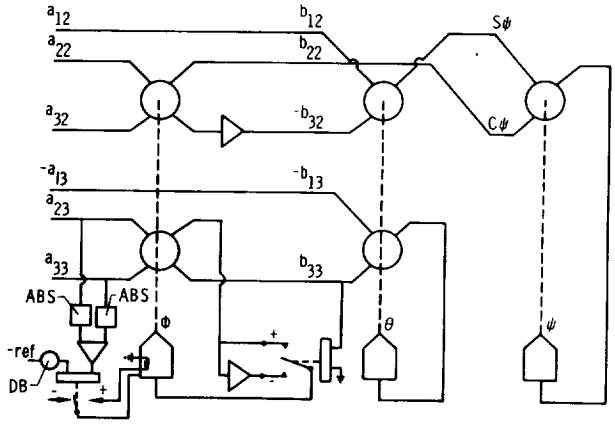

Figure 5.- Euler angle computer circuit using resolver chain with associated logic for minimization of discontinuities.

A reasonable estimate of the size of the dead band can be made by observing the effects of the dead region on the maximum angular rates. The maximum angular rate of the system is determined from equation (5) which is

$$\dot{\psi} = \frac{r \cos \phi + q \sin \phi}{\cos \theta}$$

Let the maximum slew rate attainable by the gimbal be ω_L. Then it is desired that

$$\left|\dot{\psi}\right| \leq \omega_L$$

from which (with eq. (5))

$$\theta_{db} = \left| \cos^{-1}\left[\frac{\sup(|q| + |r|)}{\omega_L}\right]\right|$$

is the value for the dead band for which rate limiting will rarely occur except for the discontinuities the magnitudes of which are minimized. This estimate does not consider the static errors inside the dead region.

THE FOUR-GIMBAL PROBLEM

Analysis

The four-gimbal configuration is shown in figure 6. It is assumed, for the purposes of the following derivations, that the transformation of coordinates, matrix A(t), is available and defined as

$$\overline{V}_r = A(t)\overline{V}_f \qquad (1)$$

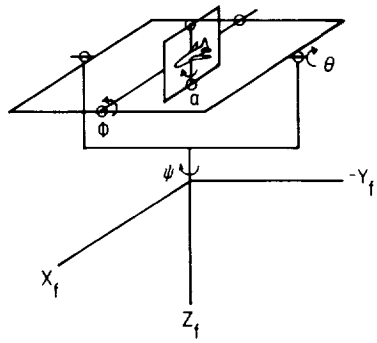

Figure 6.- Four-gimbal configuration considered in the analysis.

The transformation matrix A(t) can be constructed as a function of the four angles ψ, θ, ϕ, and α. This functional relation is

$$A(t) = [\alpha]_Z[\phi]_X[\theta]_Y[\psi]_Z \qquad (27)$$

and is expanded in equation (B1) of appendix B.

The introduction of the fourth angle makes it possible to move the singular points in the solution by the choice of the mathematical model. To demonstrate these singular properties, recall that singularities occur in the three-gimbal system when two axes are alined. Then several simple cases arise by alternately letting one of the four angles be constant. These cases are summarized in the following table:

Angle held constant	Term causing singularity
$\alpha = 0$	$\cos \theta = 0$
$\alpha = \pi/2$	$\cos \theta = 0$
$\phi = 0$	$\sin \theta = 0$
$\phi = \pi/2$	Everywhere (two gimbal)
$\theta = 0$	$\sin \phi = 0$
$\theta = \pi/2$	Everywhere (two gimbal)
$\psi = 0$	$\cos \phi = 0$
$\psi = \pi/2$	$\cos \phi = 0$

It is clear from viewing the table that many possible singularities can enter the solution. Formulations of the problem can be found that have singularities involving more than one angle, including the angles α and ψ which do not appear in the right column of the table. The problem is simplified by retaining ψ, θ, and ϕ as a general rotation from a coordinate frame that is orientated by the angle α. The singularity then arises from the one term $\cos \theta = 0$. The problem reduces to choosing α such that the singular point is never encountered.

Assume that a value for α has been chosen; thus far the choice is entirely arbitrary since four parameters overspecify the rotation of two coordinate frames (ref. 8). With this knowledge of α, a matrix D(t) can be defined as

$$D(t) = [-\alpha]_Z A(t) = [\phi]_X [\theta]_Y [\psi]_Z \tag{28}$$

These relations are expanded in equations (B2) and (B3) of appendix B. The solution for ψ, θ, and ϕ is singular at $\cos \theta = 0$ and unique in the sense of principal values for $\cos \theta > 0$. To remain an unique nonsingular solution for ψ, θ, and ϕ, the angle α must be chosen such that $\cos \theta$ remains always greater than zero.

The only difficulty left is the choice of α. Suppose that $\cos \theta$ is approaching zero; α must be changed by $\Delta\alpha$ such that the change in $\cos \theta$ (that is, $\Delta \cos \theta$) is positive. The first-order change in $\cos \theta$ with respect to α is given by

$$\Delta \cos \theta = \frac{\partial \cos \theta}{\partial \alpha} \Delta\alpha \tag{29}$$

and requiring $\cos \theta$ to increase yields

$$\frac{\partial \cos \theta}{\partial \alpha} \Delta\alpha > 0 \tag{30}$$

Since

$$\Delta\alpha \approx \dot{\alpha}\, \Delta t \tag{31}$$

Equations (31) and (32) result in

$$\frac{\partial \cos \theta}{\partial \alpha} \dot{\alpha} > 0 \tag{32}$$

Once the partial derivative is evaluated, equation (32) can be used to determine the direction to change α in order to increase $\cos \theta$.

In order to evaluate the partial derivative in inequality (32), $\cos \theta$ must be expressed as a function of α, ϕ, and t. This functional form is given by the matrix

$$C(t) = \left[-\phi\right]_X D(t) = \left[\theta\right]_Y \left[\psi\right]_Z \tag{33}$$

from which

$$c_{33} = \cos \theta = a_{13} \sin \phi \sin \alpha + a_{23} \sin \phi \cos \alpha + a_{33} \cos \phi \tag{34}$$

as seen in equations (B4) and (B5) of appendix B. Differentiating equation (34) explicitly with respect to α yields

$$\frac{\partial \cos \theta}{\partial \alpha} = a_{13} \sin \phi \cos \alpha - a_{23} \sin \phi \sin \alpha = \sin \phi (a_{13} \cos \alpha - a_{23} \sin \alpha) \tag{35}$$

From equations (B2) and (B3) of appendix B

$$d_{13} = -\sin \theta = a_{13} \cos \alpha - a_{23} \sin \alpha$$

and, hence, equation (35) becomes

$$\frac{\partial \cos \theta}{\partial \alpha} = -\sin \theta \sin \phi \tag{36}$$

From relation (32)

$$(-\sin \theta \sin \phi)\dot{\alpha} > 0 \tag{37}$$

must be maintained to insure a nonsingular solution for ψ, θ, ϕ, and α. Clearly $\dot{\alpha} \neq 0$ must be satisfied whenever $\cos \theta$ approaches zero.

Relation (37) defines the direction α must be changed to increase (maximize) $\cos \theta$. Hence, the direction is defined by $\text{sgn}(-\sin \theta \sin \phi)$ and only the magnitude is left undetermined, that is,

$$\dot{\alpha} = f(\alpha,\psi,\theta,\phi,t)\text{sgn}(-\sin \theta \sin \phi) \tag{38}$$

where $f(\theta)$ (in the sequel the arguments α, ψ, ϕ, and t are suppressed) is an arbitrary nonnegative function which is nonzero for $\cos \theta$ approaching zero. A desirable form of $f(\theta)$ can be chosen from two considerations: simplicity and the condition that $\dot{\alpha}$ goes to zero smoothly as $\cos \theta$ approaches the maximum (that is, $\sin \theta$ approaches

zero). Such a function is

$$f(\theta) = K|\sin\theta|$$

where K is a positive constant (to be determined) and this choice yields

$$\dot{\alpha} = -K \sin\theta \ \mathrm{sgn}(\sin\phi) \tag{39}$$

To investigate further the four-gimbal problem, the time derivatives of the four angles are needed. With ψ, θ, ϕ, and α used as parameters of the rotation, the rate equations are derived by transforming the angular velocity components $\dot{\psi}$, $\dot{\theta}$, $\dot{\phi}$, and $\dot{\alpha}$ into the axes of the rotating frame. The resulting angular velocity vector components are then formally equated to p, q, and r; hence,

$$\begin{bmatrix} p \\ q \\ r \end{bmatrix} = \begin{bmatrix} 0 \\ 0 \\ \dot{\alpha} \end{bmatrix} + [\alpha]_Z \begin{bmatrix} \dot{\phi} \\ 0 \\ 0 \end{bmatrix} + [\alpha]_Z[\phi]_X \begin{bmatrix} 0 \\ \dot{\theta} \\ 0 \end{bmatrix} + [\alpha]_Z[\phi]_X[\theta]_Y \begin{bmatrix} 0 \\ 0 \\ \dot{\psi} \end{bmatrix} \tag{40}$$

Expanding equation (40) gives

$$\begin{bmatrix} C\alpha & C\phi S\alpha & C\theta S\phi S\alpha - S\theta C\alpha \\ -S\alpha & C\phi C\alpha & C\theta S\phi C\alpha + S\theta S\alpha \\ 0 & -S\phi & C\theta C\phi \end{bmatrix} \begin{bmatrix} \dot{\phi} \\ \dot{\theta} \\ \dot{\psi} \end{bmatrix} = \begin{bmatrix} p \\ q \\ r - \dot{\alpha} \end{bmatrix} \tag{41}$$

Solving equation (41) for $\dot{\psi}$, $\dot{\theta}$, and $\dot{\phi}$ results in

$$\dot{\psi} = \frac{(pS\alpha + qC\alpha)S\phi + (r - \dot{\alpha})C\phi}{C\theta} \tag{42}$$

$$\dot{\theta} = (pS\alpha + qC\alpha)C\phi - (r - \dot{\alpha})S\phi \tag{43}$$

$$\dot{\phi} = (pC\alpha - qS\alpha) + S\theta\dot{\psi} \tag{44}$$

which are of a familiar functional form and where $\dot{\alpha}$ is given by equation (38) as follows:

$$\dot{\alpha} = -f(\theta)\mathrm{sgn}(\sin\theta \sin\phi)$$

In the limiting case as α and $\dot{\alpha}$ approach zero, equations (42) to (44) are the standard Euler angle rate equations given by equations (5) to (7).

Now consider the constraint inequality (eq. (37))

$$(-\sin\theta \sin\phi)\dot{\alpha} > 0$$

Substituting equation (38) into equation (37) gives

$$|\sin\theta \sin\phi| f(\theta) > 0 \tag{45}$$

If $f(\theta)$ is to be bound for $\sin\theta \neq 0$, then inequality (45) cannot be satisfied for $\sin\phi = 0$. The problem arises whether or not $\sin\phi = 0$ is a singularity. To determine the behavior at $\sin\phi = 0$, consideration must be given to the change in $\sin\phi$ due to variations in α. This change can be determined by explicit differentiation of d_{23} in equations (B2) and (B3) of appendix B where

$$d_{23} = \cos\theta \sin\phi = a_{13} \sin\alpha + a_{23} \cos\alpha$$

Differentiating gives

$$\cos\theta \frac{\partial \sin\phi}{\partial\alpha} + \sin\phi \frac{\partial \cos\theta}{\partial\alpha} = a_{13} \cos\alpha - a_{23} \sin\alpha = -\sin\theta$$

from which

$$\frac{\partial \sin\phi}{\partial\alpha} = \frac{-\sin\theta}{\cos\theta} \cos^2\phi$$

The first-order change with respect to time of $\sin\phi$ due to $\dot{\alpha}$ is

$$\frac{d}{dt}(\sin\phi) = f(\theta) \frac{|\sin\theta|}{\cos\theta} \cos^2\phi \operatorname{sgn}(\sin\phi) \tag{46}$$

which is nonzero when $\sin\theta$ and $\cos\phi$ are nonzero provided $f(\theta)$ is also nonzero. The choice of $f(\theta)$ to be nonnegative tends to maximize $|\sin\phi|$ as $|\sin\theta|$ approaches a minimum in such a way that the orientation of the coordinate systems is preserved. Hence, the choice of $f(\theta)$ to be nonzero and nonnegative when $\sin\theta$ is nonzero assures that $\sin\phi = 0$ is a saddle point (that is, the direction of $\dot{\alpha}$ is arbitrary) and not a singularity (as contrasted with results of ref. 3).

In choosing a form for $f(\theta)$, simplicity is desired to keep the complexity of the mechanization at a minimum. The choice given by equation (39), indeed, meets this requirement. Now to investigate the behavior of the system for this choice, consider a perturbation of the system

$$0 < |\theta_o| << 1 \text{ rad} \tag{47}$$

for no dynamics ($p = q = r = 0$); then equations (39) to (42) to (44) become

$$\dot{\alpha} = -K\theta \operatorname{sgn}(\sin\phi) \tag{48}$$

$$\dot{\psi} = -\cos\phi\dot{\alpha} \tag{49}$$

$$\dot{\theta} = \sin\phi\dot{\alpha} \tag{50}$$

$$\dot{\phi} = \theta\dot{\psi} \tag{51}$$

Eliminating $\dot{\psi}$ and $\dot{\alpha}$ from equations (49) to (51) gives

$$\dot{\psi} = K\theta \cos \phi \, \mathrm{sgn}(\sin \phi) \tag{52}$$

$$\dot{\theta} = -K\theta|\sin \phi| \tag{53}$$

$$\dot{\phi} = K\theta^2 \cos \phi \, \mathrm{sgn}(\sin \phi) \tag{54}$$

Note that

$$\dot{\phi} \leqq K\theta^2$$

is small since $|\theta| << 1$. Therefore assume that ϕ $(\sin \phi_0 \neq 0)$ in equations (48), (52), and (53) is constant so that the approximate solutions of these equations are, respectively,

$$\theta = \theta_0 e^{-K|\sin\phi_0|t} \tag{55}$$

$$\psi = \psi_0 + \theta_0 \frac{\cos \phi_0}{\sin \phi_0}\left(1 - e^{-K|\sin\phi_0|t}\right) \tag{56}$$

$$\alpha = \alpha_0 + \frac{\dot{\theta}_0}{\sin \phi_0}\left(e^{-K|\sin\phi_0|t} - 1\right) \tag{57}$$

Using equation (55) in equation (54) yields

$$\phi = \phi_0 + \frac{\theta_0^2}{2} \frac{\cos \phi_0}{\sin \phi_0}\left(1 - e^{-2K|\sin\phi_0|t}\right)$$

It is seen from the form of these approximate solutions that $1/\left(K|\sin \phi_0|\right)$ assumes the role of a relaxation time. The dependence of the relaxation time on $\sin \phi$ is not a serious problem, provided K is chosen to be sufficiently large, since $|\sin \phi|$ is "maximized."

Since this solution was nondynamical, the space orientation of the two coordinate frames is unchanged. The slight perturbation induces motion, in general, in all the gimbal angles such that the orientation is preserved. Hence, the angles are not unique for any given orientation. The gain constant K has been related to the relaxation time. This relaxation time must be sufficiently small to allow the gimbal servodrives to respond. In the following discussion, an upper limit for K is found from this consideration. In addition, a lower limit for K is established for the dynamic case to maintain a nonsingular solution.

Let ω_L be the maximum obtainable slew rate of the gimbal system. For the nondynamic case, it is seen from equations (48) to (51) that each angular rate is less than or

equal to $|\dot{\alpha}|$, where

$$|\dot{\alpha}| = K|\sin\theta| \tag{58}$$

Clearly the choice

$$K < \frac{\omega_L}{|\sin\theta_{max}|} \tag{59}$$

where θ_{max} is the largest attainable value of $|\theta|$, will limit nondynamically all the gimbal angle rates to within the gimbal system tolerances.

To make a dynamic estimate, consider equation (43). Basic to the derivation of the four-gimbal problem is the assumption that a value of $\dot{\alpha}$ can be found such that $\cos\theta$ always remains large. It is then obvious that the $\dot{\alpha}$ term must have the dominant magnitude of all the terms in equation (43) for some θ not zero; visually

$$|\dot{\alpha}\sin\phi| > |(p\sin\alpha + q\cos\alpha)\cos\phi - r\sin\phi| \tag{60}$$

This inequality would be difficult to justify rigorously; however, in view of equation (46), inequality (60) is at least plausible. Since the sine and cosine are magnitude bound by unity, then

$$|p| + |q| + |r| > |(p\sin\alpha + q\cos\alpha)\cos\phi - r\sin\phi|$$

and

$$|\dot{\alpha}| = K|\sin\theta| \geq |\dot{\alpha}\sin\phi|$$

Therefore the choice (for some $\theta \neq 0$)

$$K|\sin\theta| > |p| + |q| + |r| \tag{61}$$

insures a nonsingular formulation, under the assumption of plausibility of inequality (60). Let

$$\beta = \sup\left(|p|,|q|,|r|\right)$$

Then the choice

$$K > \frac{3\beta}{|\sin\theta_{max}|} \tag{62}$$

insures inequality (61) for some value of β and, hence, insures a nonsingular problem.

Combining inequalities (59) and (62) yields

$$\frac{3\beta}{|\sin\theta_{max}|} < K < \frac{\omega_L}{|\sin\theta_{max}|}$$

The value θ_{max} is the upper limit for those values of $|\theta|$ for which inequality (60) is not valid; that is, the $\dot{\alpha}$ term is not sufficiently large to increase $\cos\theta$ or,

alternately, decrease $|\theta|$. For values of $|\theta|$ on the order of θ_{max}, the $\dot{\alpha}$ term is dominant and $|\theta|$ decreases. Hence, θ_{max} is a limiting value for $|\theta|$.

In choosing a value for θ_{max}, consideration must be given to the singular point in equation (42). The value for θ_{max} must be sufficiently far from the singular point so that excessive rates do not occur. A reasonable choice would be $\sin \theta_{max} = 0.75$ from which

$$4\beta < K < \frac{4\omega_L}{3}$$

This range for K will maintain a nonsingular solution since

$$|\theta| < \frac{1}{3}\pi$$

and the maximum angular rates should not tax the capabilities of the gimbal systems.

Application

The problem of computing for ψ, θ, ϕ, and α is formally solved by using equation (39), in conjunction with the matrix elements c_{13}, c_{21}, c_{22}, c_{33}, d_{23}, and d_{33} of equations (28) and (33). The resulting equations (with eq. (39) included) are

$$\dot{\alpha} = -K \sin \theta \operatorname{sgn}(\sin \phi)$$

$$\sin \phi = \frac{(a_{13} \sin \alpha + a_{23} \cos \alpha)}{\cos \theta} \tag{63}$$

$$\cos \phi = \frac{a_{33}}{\cos \theta} \tag{64}$$

$$\sin \psi = a_{31} \sin \phi - (a_{11} \sin \alpha + a_{21} \cos \alpha)\cos \phi \tag{65}$$

$$\cos \psi = (a_{12} \sin \alpha + a_{22} \cos \alpha)\cos \phi - a_{32} \sin \phi \tag{66}$$

$$\sin \theta = a_{23} \sin \alpha - a_{13} \cos \alpha \tag{67}$$

$$\cos \theta = (a_{13} \sin \alpha + a_{23} \cos \alpha)\sin \phi + a_{33} \cos \phi \tag{68}$$

This solution for ψ, θ, ϕ, and α is algebraic with the exception of $\dot{\alpha}$.

The computation of ψ, θ, ϕ, and α can also be accomplished by solving the differential equations (39) and (42) to (44). This solution is equivalent, neglecting computation error, to the algebraic solution.

Mechanization

Only the mechanization of the algebraic formulation is considered. The matrix D(t) has the functional form of the three-gimbal problem previously discussed. Hence, the computer circuit in figure 5, with the logic deleted, can be used to solve this matrix. From figure 5, the elements

$$\left.\begin{aligned} d_{12} &= a_{12}C\alpha - a_{22}S\alpha \\ d_{22} &= a_{12}S\alpha + a_{22}C\alpha \\ d_{32} &= a_{32} \\ d_{13} &= a_{13}C\alpha - a_{23}S\alpha \\ d_{23} &= a_{13}S\alpha + a_{23}C\alpha \\ d_{33} &= a_{33} \end{aligned}\right\} \tag{69}$$

are needed to compute the angles ψ, θ, and ϕ. Since

$$\operatorname{sgn}(\sin\phi) = \operatorname{sgn}(\phi)$$

a low-accuracy linear or sine potentiometer on the ϕ shaft can be used in conjunction with d_{13} to compute $\dot{\alpha}$. For the linear potentiometer

$$\dot{\alpha} = +Kd_{13}\operatorname{sgn}(\phi) \tag{70}$$

Using an integrating servomotor results in the mechanization shown in figure 7.

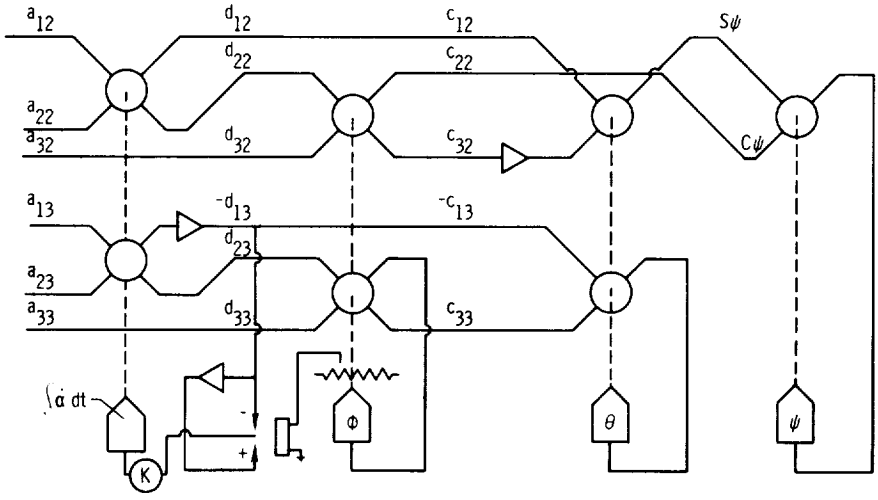

Figure 7.- Computer circuit using resolver chain for the computation of the essentially algebraic formulation of the four-gimbal problem.

RESULTS AND DISCUSSION

The computer circuit in figure 5 was programed on an analog computer with A(t) generated by the Euler parameter rate equations given in appendix A.

The Euler angle rate equations admit continuous solutions for constant p, q, and r; this is seen from the right- and left-hand limits of equation (13) which has two principal solutions at each limit which are equal. Thus, continuous pitch capability is possible provided the solution with $\Delta\phi = 0$ is chosen. The other solution has $\Delta\phi = \pi$ (eq. (14)). The logic shown in figure 5 only allows the continuous solutions. If the ratio of q and r is changed at the singular points, then discontinuities will result. The logic in figure 5 minimizes the magnitudes of these discontinuities.

If a singular point is approached but not encountered, the solutions are continuous but the angular rates are exceedingly high. Such a solution is shown in figure 8. This solution was obtained by initiating a small roll maneuver ($\phi = 3^{o}$) followed by a pitchover ($q > 0$) and return ($q < 0$). The solution in this figure was obtained from the circuit in figure 5 with the logic disabled.

If the logic in figure 5 is enabled, then the high rates over the large change in the angles ψ and ϕ, shown in figure 8, are replaced by small discontinuities. The same solution is shown in figure 9 with the logic enabled (the dead band was chosen to be exceedingly large, $\approx 20^{o}$, in order to demonstrate clearly the nature of the solution, whereas typically the dead band is chosen to be from 2^{o} to 5^{o}). These high rate solutions could result in rate limiting of mechanical equipment which may cause serious degradation of the visual display. The small discontinuities are not believed to be as serious a limitation because of the relatively small distances over which rate limiting does occur (a smaller dead band would decrease the size of the discontinuity shown in fig. 9).

The method of enhancing three-gimbal systems may be adequate for many simulation problems. When fast gimbal systems are available and low accuracy is sufficient around the singular points, a three-gimbal system is often suitable, especially in view of the cost difference between a three- and a four-gimbal system. Associated with the dead band is a static

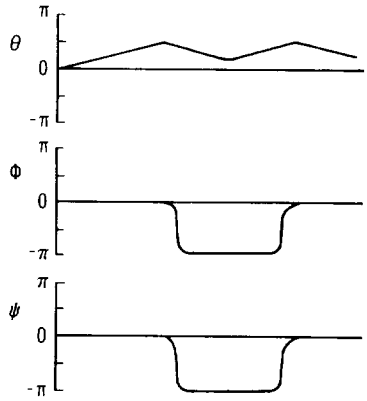

Figure 8.- Solution for pitchover and return with an initial small roll angle.

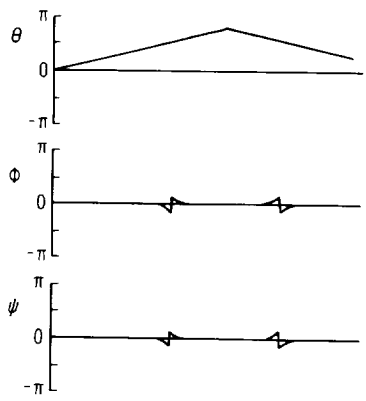

Figure 9.- Approximate solution for pitchover and return with an initial small roll angle.

error which results in a pointing inaccuracy that is less than or equal to the dead-band size. If a pointing measurement must be made near the singular point, then the dead band must be made as small as possible to reduce the static error. However, the dynamic error will increase and one must decide from the simulation requirements what is acceptable.

Equations (39) and (63) to (68) for the four-gimbal system were programed on an analog computer with the matrix A(t) again generated by the Euler parameter rate equations. A pitchover was executed with K = 2, 4, and 6; the results are shown in figures 10, 11, and 12, respectively. These solutions have $\sin \phi = 0$ initially, which is the saddle point of the inequality constraint. As seen in these figures, the resultant motion is entirely absorbed in the ϕ-axis of the gimbal. Pitchover with $\sin \phi = 0$ initially is where "gimbal flip" should occur according to reference 3.

It appears from the maximum values of $\dot{\alpha}$ in figures 10, 11, and 12 that K = 2 is adequate when the components of the angular velocity vector are less than or equal to 1/2 radian per second. Note that this value of K is 4β, the lower limit established for K. With this lower limit, the solution for various inputs p, q, and r is shown in figure 13. Again, there is no indication of misbehavior.

Because Euler angles are needed in many simulation problems, several special-purpose analog computers have been constructed with circuits which closely resemble that in figure 5. These computers eliminate the task of reprograming the equations for the Euler angles of each simulation problem. Furthermore, they conserve the quantity

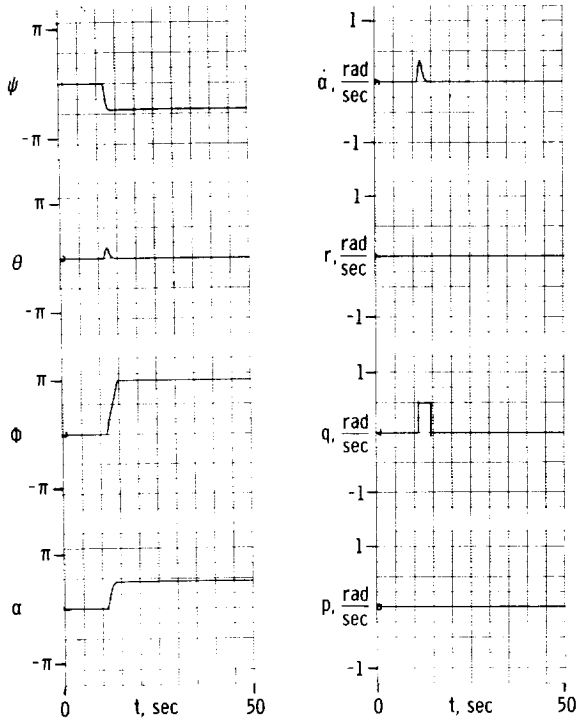

Figure 10.- Pitchover for the four-gimbal model with K = 2.

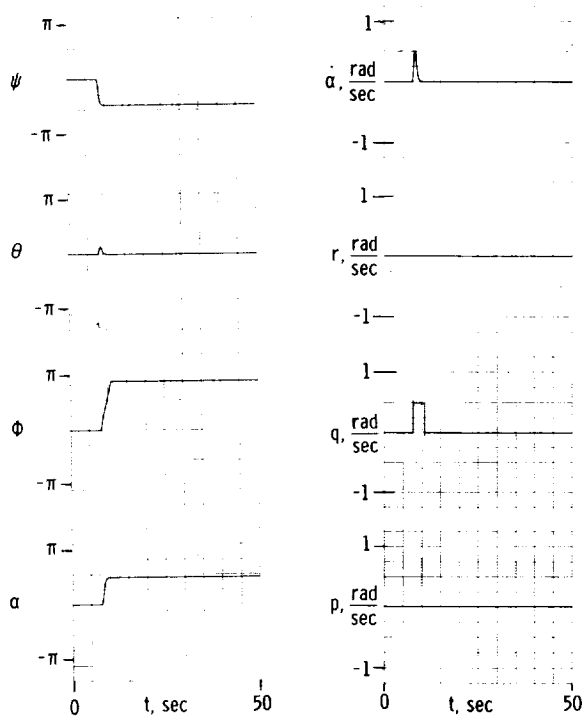

Figure 11.- Pitchover for the four-gimbal model with K = 4.

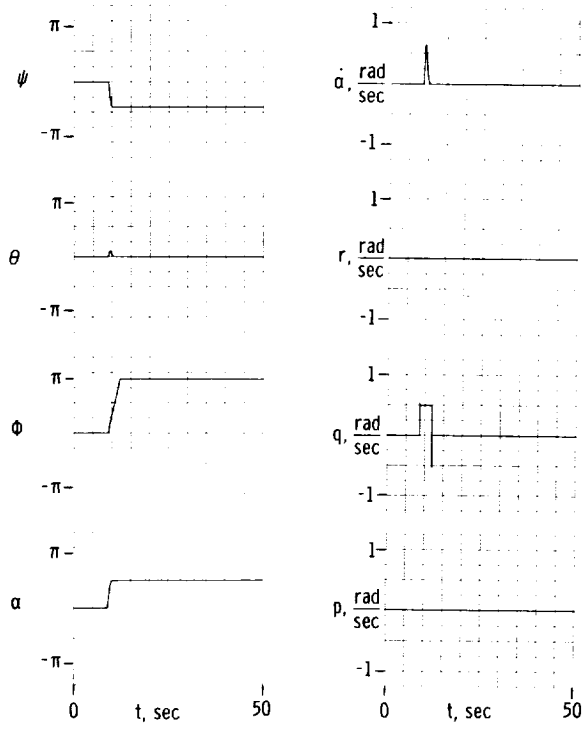

Figure 12.- Pitchover for the four-gimbal model with K = 6.

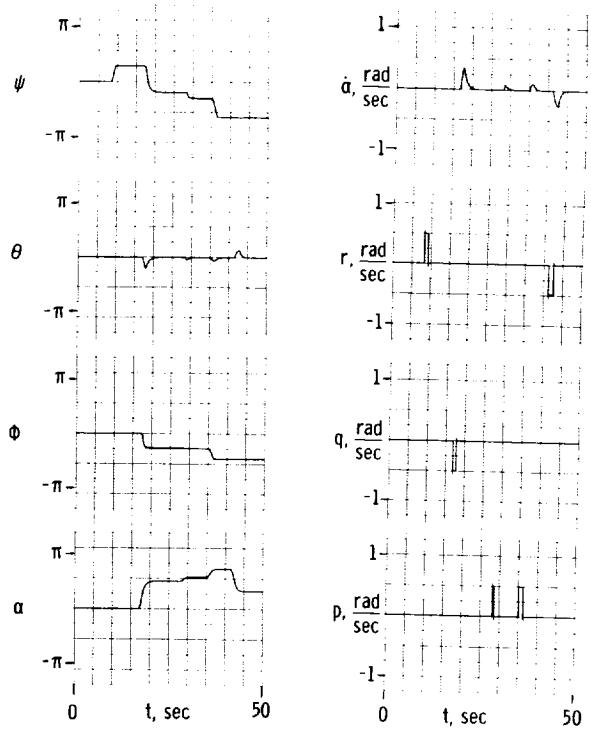

Figure 13.- Solution of four-gimbal model with K = 2 for indicated inputs.

required of the general purpose simulation computer. Reducing the general purpose simulation computer requirements is especially important in digital simulation where the resolution of Euler angles often requires as much or more computation time as does the remaining portion of the simulation problem. The Euler angle computer is reprogrammable for different orders of rotation by simply matching the functional forms of the input direction cosines.

To solve for the four-gimbal angles, the construction of a special-purpose computer, based on figure 7, is being planned. The computer for four-gimbal systems has an added advantage in that it can be used in a three-gimbal mode by bypassing the α resolver. Previous all-attitude indicators have been proposed and developed with both the three- and four-gimbal concepts used. (See, for example, refs. 3, 4, 9, and 10.) For the three-gimbal systems proposed and developed, there is some disagreement about the way in which a three-gimbal attitude display should operate. The solutions of minimum discontinuity are indicated in references 4 and 9, and those of maximum discontinuity are indicated in reference 10.

A four-gimbal inertial platform (fig. 14) is proposed in reference 4 so that "there is no possibility of gimbal lock." The proposed mechanization is to operate with the following constraint: "A pick-off device, mounted between the first and second gimbal rings

at the axis of support of the first gimbal ring, causes the third gimbal to be driven in such a manner that the first and second gimbal rings maintain an orthogonal relationship during any possible aircraft maneuver." This constraint is not to be taken literally. It is to be noted that this four-gimbal system drives a three-gimbal all-attitude display (8-ball). The proposed system (according to ref. 4) "lacks sensitivity within two or three degrees of the vertical" and thus requires a "pitch indicator follow-up system" so that a change in heading "is shown as soon as it occurs" in this "exceptional case."

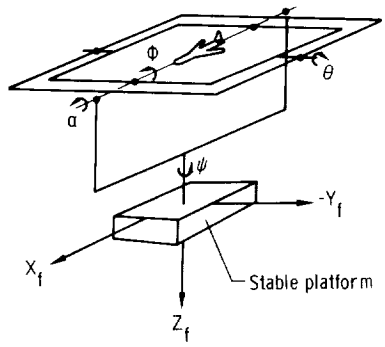

Figure 14.- Four-gimbal system used with stable platform. (See ref. 3.)

This same gimbal configuration is again reported in reference 3, page 130, where the problems in the exceptional case are more clearly discussed: ". . . the fourth gimbal must "flip" or rotate 180 degrees as pitch angle passes through 90 degrees."

The four-gimbal systems discussed in references 3 and 4 are analyzed in appendix C. The difficulty in all these systems is encountered when

$$\frac{\partial \cos \alpha}{\partial \phi} = \cos \theta \sin \alpha = 0$$

which was shown to be a saddle point (and need not be a singular point as indicated by ref. 3) if a proper form for $\dot{\phi}$ is chosen, namely,

$$\dot{\phi} = f(\alpha)\text{sgn}(\cos \theta \sin \alpha)$$

It appears that a slight alteration could greatly enhance these existing four-gimbal systems.

CONCLUDING REMARKS

The technique described in this paper extends the usefulness of the many existing three-gimbal systems by providing a method of handling solutions at the singular points (gimbal lock) in a predictable and desirable manner. Even so, the quality of motion in the neighborhood of the singular points obtainable from a three-gimbal system may not be sufficient for all applications. For example, a static error introduced in the solution may be as large as the dead band (2^o to 5^o).

A four-gimbal system can entirely eliminate discontinuities. The experimental results from the four-gimbal model indicate no adverse behavior. Due to the non-uniqueness of the angles, error in the computations of the fourth angle does not affect the

static or dynamic accuracy of the gimbal system when the essentially algebraic formulation is used.

It appears that an improved version of a four-gimbal stabilized platform could be built by applying the results of this investigation. Clearly, the need for a feasibility study is indicated by the analysis.

The two special-purpose analog computers for solving the three- and four-gimbal problems provide a cost advantage by reducing programing time and the demands placed on general-purpose computing equipment.

Langley Research Center,
National Aeronautics and Space Administration,
Langley Station, Hampton, Va., March 14, 1968,
125-19-06-02-23.

APPENDIX A

THREE-GIMBAL MATHEMATICAL DETAIL

The matrix A(t) is found (ref. 8) as a function of the Euler parameters (a normalized quaternion) by

$$A(t) = \begin{bmatrix} 2(a^2 + d^2) - 1 & 2(ab - cd) & 2(ac + bd) \\ 2(ab + cd) & 2(b^2 + d^2) - 1 & 2(cb - ad) \\ 2(ac - bd) & 2(cb + ad) & 2(c^2 + d^2) - 1 \end{bmatrix} \tag{A1}$$

where

$$\left.\begin{aligned} \dot{a} &= \frac{1}{2}(-pd - qc + rb) \\ \dot{b} &= \frac{1}{2}(pc - qd - ra) \\ \dot{c} &= \frac{1}{2}(-pb + qa - rd) \\ \dot{d} &= \frac{1}{2}(pa + qb + rc) \end{aligned}\right\} \tag{A2}$$

and p, q, and r are the components of the angular velocity vector measured along the rotating coordinate axis.

Expanding A(t) as a function of the three Euler angles ψ, θ, and ϕ results in

$$A(t) = [\phi]_X[\theta]_Y[\psi]_Z = \begin{bmatrix} (C\psi C\theta) & (S\psi C\theta) & (-S\theta) \\ \begin{pmatrix} C\psi S\theta S\phi \\ -S\psi C\phi \end{pmatrix} & \begin{pmatrix} C\psi C\phi \\ +S\phi S\psi S\theta \end{pmatrix} & (S\phi C\theta) \\ \begin{pmatrix} S\psi S\phi \\ +C\phi C\psi S\theta \end{pmatrix} & \begin{pmatrix} C\phi S\psi S\theta \\ -S\phi C\psi \end{pmatrix} & (C\phi C\theta) \end{bmatrix} \tag{A3}$$

APPENDIX A

Provided ϕ is known, a matrix B(t) can be computed as

$$B(t) = [-\phi]_X A(t) = \begin{bmatrix} a_{11} & a_{12} & a_{13} \\ (a_{21}C\phi - a_{31}S\phi) & (a_{22}C\phi - a_{32}S\phi) & (a_{23}C\phi - a_{33}S\phi) \\ (a_{21}S\phi + a_{31}C\phi) & (a_{22}S\phi + a_{32}C\phi) & (a_{23}S\phi + a_{33}C\phi) \end{bmatrix} \quad \text{(A4)}$$

where B(t) is functionally related to θ and ψ by

$$B(t) = [\theta]_Y[\psi]_Z = \begin{bmatrix} C\psi C\theta & S\psi C\theta & -S\theta \\ -S\psi & C\psi & 0 \\ C\psi S\theta & S\psi S\theta & C\theta \end{bmatrix} \quad \text{(A5)}$$

APPENDIX B

FOUR-GIMBAL MATHEMATICAL DETAIL

Expanding $A(t)$ as a function of the four gimbal angles ψ, θ, ϕ, and α yields

$$A(t) = [\alpha]_Z [\phi]_X [\theta]_Y [\psi]_Z = \begin{bmatrix} \begin{pmatrix} C\alpha C\psi C\theta \\ +S\alpha C\psi S\theta S\phi \\ -S\alpha S\psi C\phi \end{pmatrix} & \begin{pmatrix} C\alpha S\psi C\theta \\ +S\alpha C\psi C\phi \\ -S\alpha S\phi S\psi S\theta \end{pmatrix} & \begin{pmatrix} -S\theta C\alpha \\ +S\alpha C\theta S\phi \end{pmatrix} \\ \begin{pmatrix} C\alpha C\psi S\theta S\phi \\ -C\alpha S\psi C\phi \\ -S\alpha C\psi C\theta \end{pmatrix} & \begin{pmatrix} C\alpha C\psi C\phi \\ +C\alpha S\phi S\psi S\theta \\ -S\alpha S\psi C\theta \end{pmatrix} & \begin{pmatrix} S\theta S\alpha \\ +S\phi C\theta C\alpha \end{pmatrix} \\ \begin{pmatrix} S\psi S\phi \\ +C\phi C\psi S\theta \end{pmatrix} & \begin{pmatrix} C\phi S\psi S\theta \\ -S\phi C\psi \end{pmatrix} & (C\phi C\theta) \end{bmatrix} \tag{B1}$$

With a knowledge of α, the matrix $D(t)$ is

$$D(t) = [-\alpha]_Z A(t) = \begin{bmatrix} (a_{11}C\alpha - a_{21}S\alpha) & (a_{12}C\alpha - a_{22}S\alpha) & (a_{13}C\alpha - a_{23}S\alpha) \\ (a_{11}S\alpha + a_{21}C\alpha) & (a_{12}S\alpha + a_{22}C\alpha) & (a_{13}S\alpha + a_{23}C\alpha) \\ a_{31} & a_{32} & a_{33} \end{bmatrix} \tag{B2}$$

The matrix $D(t)$ as a function of the three angles ψ, θ, and ϕ is given by

$$D(t) = [\phi]_X [\theta]_Y [\psi]_Z = \begin{bmatrix} (C\psi C\theta) & (S\psi C\theta) & (-S\theta) \\ \begin{pmatrix} C\psi S\theta S\phi \\ -S\psi C\phi \end{pmatrix} & \begin{pmatrix} C\psi C\phi \\ +S\phi S\psi S\theta \end{pmatrix} & (S\phi C\theta) \\ \begin{pmatrix} S\psi S\phi \\ +C\phi C\psi S\theta \end{pmatrix} & \begin{pmatrix} C\phi S\psi S\theta \\ -S\phi C\psi \end{pmatrix} & (C\phi C\theta) \end{bmatrix} \tag{B3}$$

The solution for ψ, θ, and ϕ from equation (B3) is well known.

APPENDIX B

Again, C(t) is found to be a function of A(t), α, and ϕ as

$$C(t) = [-\phi]_X[-\alpha]_Z A(t) = \begin{bmatrix} (a_{11}C\alpha - a_{21}S\alpha) & (a_{12}C\alpha - a_{22}S\alpha) & (a_{13}C\alpha - a_{23}S\alpha) \\ \begin{matrix}(a_{11}C\phi S\alpha + a_{21}C\phi C\alpha)\\ -a_{31}S\phi\end{matrix} & \begin{matrix}(a_{12}C\phi S\alpha + a_{22}C\phi C\alpha)\\ -a_{32}S\phi\end{matrix} & \begin{matrix}(a_{13}C\phi S\alpha + a_{23}C\phi C\alpha)\\ -a_{33}S\phi\end{matrix} \\ \begin{matrix}(a_{11}S\phi S\alpha + a_{21}S\phi C\alpha)\\ +a_{31}C\phi\end{matrix} & \begin{matrix}(a_{12}S\phi S\alpha + a_{22}S\phi C\alpha)\\ +a_{32}C\phi\end{matrix} & \begin{matrix}(a_{13}S\phi S\alpha + a_{23}S\phi C\alpha)\\ +a_{33}C\phi\end{matrix} \end{bmatrix} \quad \text{(B4)}$$

or of θ and ψ as

$$C(t) = [\theta]_Y[\psi]_Z = \begin{bmatrix} C\psi C\theta & S\psi C\theta & -S\theta \\ -S\psi & C\psi & 0 \\ C\psi S\theta & S\psi S\theta & C\theta \end{bmatrix} \quad \text{(B5)}$$

APPENDIX C

ANALYSIS OF SOME EXISTING FLIGHT SYSTEMS

For the four-gimbal configuration shown in figure 14, the transformation from the fixed to the rotating frame is given by

$$\overline{V}_r = [\phi]_X[\theta]_Y[\alpha]_X[\psi]_Z\overline{V}_f = A(t)\overline{V}_f \tag{C1}$$

The angle ϕ must be chosen such that α is not allowed to approach $\pm 90^o$ (that is, $\cos \alpha$ must not be zero). Hence, the necessary constraint is

$$\frac{\partial \cos \alpha}{\partial \phi} \dot{\phi} > 0 \tag{C2}$$

where $\dot{\phi}$ must not be zero whenever $\cos \alpha$ differs from 1. The expression of $\cos \alpha$ as a function of $A(t)$, ψ, θ, and ϕ is found from the following matrix equation:

$$B(t) = [\alpha]_X[\psi]_Z = [-\theta]_Y[-\phi]_X A(t) \tag{C3}$$

from which

$$b_{33} = \cos \alpha = -a_{13} \sin \theta + \cos \theta\left(a_{23} \sin \phi + a_{33} \cos \phi\right) \tag{C4}$$

The partial derivative in equation (C2) is then

$$\frac{\partial \cos \alpha}{\partial \phi} = \cos \theta\left(a_{23} \cos \phi - a_{33} \sin \phi\right) \tag{C5}$$

Use is then made of

$$b_{23} = \sin \alpha = a_{23} \cos \phi - a_{33} \sin \phi \tag{C6}$$

from which

$$\frac{\partial \cos \alpha}{\partial \phi} = \cos \theta \sin \alpha \tag{C7}$$

The choice for $\dot{\phi}$ is then

$$\dot{\phi} = f(\alpha)\text{sgn}(\cos \theta \sin \alpha) \tag{C8}$$

where $f(\alpha)$ is a positive bounded function that is nonzero for $\cos \alpha \neq 1$.

The form for $\dot{\phi}$ as indicated by references 3 and 4 is

$$\dot{\phi} = f(\alpha)\ \text{sgn}(\alpha)$$

which is insufficient to maintain a nonsingular formulation. Note that "gimbal flip" and the "exceptional case" occur when $\cos \theta$ changes sign.

REFERENCES

1. Rogers, A. E.; and Connolly, T. W.: Analog Computation in Engineering Design. McGraw-Hill Book Co., Inc., 1960.

2. Mitchell, E. E. L.; and Rogers, A. E.: Quaternion Parameters in the Simulation of a Spinning Rigid Body. Simulation, vol. 4, no. 6, June 1965, pp. 390-396.

3. Parvin, Richard H.: Inertial Navigation. Principles of Guided Missile Design, Grayson Merrill, ed., D. Van Nostrand Co., Inc., c.1962.

4. Arnold, J. W.; and Schlesinger, H.: Two Display Designs for Presentation of All Flight Attitudes. WADC Tech. Rep. 54-316, U.S. Air Force, July 1954. (Available from DDC as AD No. 95417.)

5. Buck, R. Creighton: Advanced Calculus. McGraw-Hill Book Co., Inc., 1956.

6. Greenwood, D. T.: An Extended Euler Angle Coordinate System for Use With All-Attitude Aircraft Simulators. WADD Tech. Rep. 60-372, U.S. Air Force, Aug. 1960.

7. Godet, Sidney: Solving 3-D Problems Made Simple by Stereographic Projection – II. Space/Aeronaut., vol. 33, no. 6, June 1960, pp. 114-118.

8. Stuelpnagel, John: On the Parametrization of the Three-Dimensional Rotation Group. Contracts AF 49(638)-1242, NASw-845, and Nonr-3693(00), RIAS Div., Martin Co., 1948.

9. Anast, James: Advanced Cockpit Instrumentation. AGARD Rep. 235, May 1959.

10. Fraser, W. F.: Evaluation of the Horizontal Situation Indicator and All-Attitude and Heading Reference Indicator. ST312-60 (PTR AV-37001), U.S. Naval Air Test Center (Patuxent River, Md.), Feb. 18, 1960.